Inorganic Chemistry

ARTICLE

pubs.acs.org/IC

Electrogenerated Chemiluminescence of Platinum(II) Alkynyl Terpyridine Complex with Peroxydisulfate as Coreactant

Zuofeng Chen, Keith Man-Chung Wong, Eric Chi-Ho Kwok, Nianyong Zhu, Yanbing Zu, and Vivian Wing-Wah Yam*

Institute of Molecular Functional Material and Department of Chemistry, The University of Hong Kong, Pokfulam Road, Hong Kong, P.R. China

Supporting Information

ABSTRACT: A Pt(II) alkynyl terpyridine complex containing a carbazole moiety, $[Pt(^tBu_3tpy)(C{\equiv}C{-}C_6H_4\text{-}4\text{-carbazole-}9)]^+$ ($^tBu_3tpy$ = 4,4′,4″-tri-*tert*-butyl-2,2′:6′,2″-terpyridine) **1**, has been synthesized and characterized. The photophysical behavior has been studied, and the molecular structure has been determined by X-ray crystallography. The complex was found to exhibit intense electrogenerated chemiluminescence (ECL) using peroxydisulfate ($S_2O_8^{2-}$) as coreactant in acetonitrile/water (1−25%, v/v) mixture at both glassy carbon and gold electrodes, representing the first ECL example of the Pt(II) alkynyl family. The ECL was produced at potential corresponding to the first reduction wave (−0.90 V vs SCE), significantly shifted by ∼0.65 V toward more positive potential compared with that of $[Ru(bpy)_3]^{2+}$ (bpy = 2,2′-bipyridine). The ECL spectrum was found to be identical to the photoluminescence spectrum recorded in the same medium, indicating the formation of the same excited state of $d\pi(Pt) \rightarrow \pi^*(^tBu_3tpy)$ ^{3}MLCT mixed with $\pi(C{\equiv}CR) \rightarrow \pi^*(^tBu_3tpy)$ ^{3}LLCT in both cases. The ECL mechanism was proposed involving the formation of the strongly oxidizing intermediate, $SO_4^{\bullet-}$, mainly generated during the catalytic reduction of $S_2O_8^{2-}$ by the electrogenerated $\mathbf{1}^-$. Chemiluminescence of $\mathbf{1}/S_2O_8^{2-}$ based on reduction with Al metal is also described.

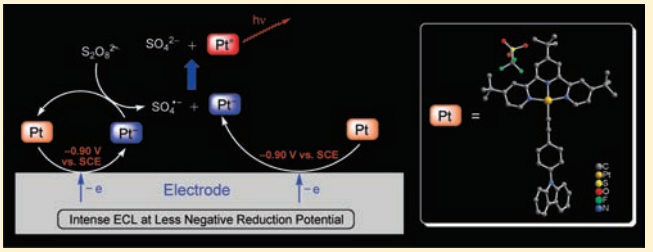

INTRODUCTION

Electrogenerated chemiluminescence (ECL) involves the formation of excited state species as a result of highly energetic electron-transfer reactions of reactants formed electrochemically.[1] While ECL of transition metal polypyridine complexes, and in particular $[Ru(bpy)_3]^{2+}$ (bpy = 2,2′-bipyridine), has attracted interest from both theoretical and practical points of view, coreactants have played a key role in promoting ECL as a powerful analytical technique for the biologically important aqueous system.[1] In a coreactant ECL system, the emission is produced upon a single potential step or sweep. This is in contrast to the annihilation system, which requires a double-potential step (e.g., oxidation followed by reduction, or vice versa) and is usually conducted in rigorously purified and deoxygenated non-aqueous media, because the available potential range in water is too narrow to generate the required energetic precursors. "Oxidative-reductive" coreactants such as tri-*n*-propylamine (TPrA)[2] and oxalate ($C_2O_4^{2-}$),[3] and "reductive-oxidative" coreactants such as peroxydisulfate ($S_2O_8^{2-}$),[4] are usually employed as the reactants that could form strong reducing or oxidizing agents upon electrochemical oxidation or reduction. In comparison to the substantial amount of studies of the $[Ru(bpy)_3]^{2+}$/TPrA ECL system,[2,5] much less attention has been paid to the peroxydisulfate "reductive-oxidative" coreactant ECL system.[4]

The first "reductive-oxidative" coreactant ECL reactions were introduced independently by the groups of Bolletta[4a] and Bard[4b] in 1982. During the reduction process, $S_2O_8^{2-}$ was reduced to the strong oxidant $SO_4^{\bullet-}$, which has a redox potential of $E^o \geq +3.15$ V versus SCE.[6] The ECL production in acetonitrile (MeCN) and aqueous solution by reaction of electrogenerated $[Ru(bpy)_3]^+$, $[Cr(bpy)_3]^{2+}$, or $[Os(bpy)_3]^+$ with the strongly oxidizing $SO_4^{\bullet-}$ intermediate generated during the reduction of $S_2O_8^{2-}$ was described by Bolletta et al.[4a] Because $[Ru(bpy)_3]^+$ ($E^o([Ru(bpy)_3]^{2+/+}) = \sim -1.46$ V vs SCE)[7] is unstable in aqueous solutions and peroxydisulfate salt has a low solubility in MeCN, the MeCN/H_2O (1/1, v/v) mixed solvent system was employed by Bard and co-workers to produce intense ECL emission.[4b]

ECL studies of some other metal complexes, including $[Mo_2Cl_4(PMe_3)_4]$,[8] Eu(III),[9] $[Ru(bpy)_2(bphb)]^{2+}$ [bphb = 1,4-bis(4′-methyl-2,2′-bipyridine-4-yl)benzene],[10] $[\{(bpy)_2Ru\}_2(bphb)]^{4+}$,[10] $[Ru(phen)_3]^{2+}$ (phen =1,10-phenanthroline),[11] $Pt_2(P_2O_5H_2)_4^{4-}$ chelate,[12a] and $Pt(Thpy)_2$ (Thpy =2-(2-thienyl)-2-pyridine)[12b] using $S_2O_8^{2-}$ as a coreactant have also been reported. These complexes usually also possess fairly negative reduction potentials, or the ECL intensities are orders of magnitude lower than that of the reported $[Ru(bpy)_3]^{2+}$ systems, limiting their practical use in analytical applications.

A promising example of the $S_2O_8^{2-}$ coreactant ECL system was reported on $[Ru(bpz)_3]^{2+}$ (bpz = 2,2′-bipyrazine),[13] which is an analogue of $[Ru(bpy)_3]^{2+}$. The redox potentials for

Received: June 3, 2010
Published: February 22, 2011

$[Ru(bpz)_3]^{2+}$ are shifted by about 0.5 V toward more positive potential compared with those for $[Ru(bpy)_3]^{2+}$. Such a positive shift of the redox potentials has facilitated electrochemical and photoelectrochemical studies of $[Ru(bpz)_3]^{2+}$ in the negative potential range in water, because the interference due to the proton reduction that takes place at negative potentials could be avoided.

Square-planar platinum(II) complexes, especially those with polypyridyl ligands, have been extensively investigated in view of their rich photoluminescence properties.[14−21] Apart from the photophysical studies, platinum(II) complexes with square-planar geometry have attracted considerable attention as a result of their interesting biological activities, such as antitumor cytotoxicity,[16] DNA intercalation,[16c−e,17] and protein binding behavior.[18] At the same time, the electrochemistry of the alkynylplatinum(II) polypyridyl complexes has also been studied, which revealed well-defined redox behaviors.[19a,g] Despite examples on the use of this class of platinum(II) complexes as luminescent labeling reagents for biomolecules being known,[15g,h,19g] the utilization of the square-planar platinum(II) polypyridyl system for ECL has been rare.[12b]

In this paper, we describe the photophysical and electrochemical studies of a Pt(II) alkynyl terpyridine complex, $[Pt(^tBu_3tpy)(C{\equiv}C{-}C_6H_4\text{-}4\text{-carbazole-}9](OTf)$ ($^tBu_3tpy$ =4,4′,4″-tri-*tert*-butyl-2,2′:6′,2″-terpyridine) **1** (Scheme 1), and demonstrate the production of ECL and its characteristics using $S_2O_8^{2-}$ as the coreactant. A bright orange luminescence could be observed by reducing **1** and $S_2O_8^{2-}$ at potentials where hydrogen evolution is not appreciable. The ECL intensity of the $\mathbf{1}/S_2O_8^{2-}$ system was found to be a function of $S_2O_8^{2-}$ concentration and be affected by experimental factors, such as the nature of the solvent, pH, and electrode materials. The possible pathway for the ECL of the $\mathbf{1}/S_2O_8^{2-}$ system was proposed. A chemiluminescence of $\mathbf{1}/S_2O_8^{2-}$ based on reduction with Al metal is also described.

EXPERIMENTAL SECTION

Chemicals. Potassium peroxydisulfate ($K_2S_2O_8$), and tetra-*n*-butylammonium hexefluorophosphate ($^nBu_4NPF_6$, ≥ 99%) were purchased from Sigma-Aldrich. 9-(4-Ethynylphenyl)carbazole was synthesized and purified according to the literature procedures.[22] Other chemicals were of analytical grade and were used as received. All aprotic solvents were purified and distilled using standard procedures before use. All the aqueous solutions were prepared with deionized water (Milli-Q, Millipore). The pH of the phosphate buffer (PB, 0.15 M) solution was adjusted with concentrated NaOH or phosphoric acid. The stock solution of **1** (1 mM) was prepared in MeCN, followed by dilution (100-fold, v/v) with MeCN or MeCN/H_2O mixture for the photoluminescence (PL) and ECL measurements.

Synthesis. 9-(4-Ethynylphenyl)carbazole (88 mg, 0.33 mmol), a catalytic amount of CuI (2 mg, 5%), and NEt_3 (1 mL) were added to a degassed solution of $[Pt(^tBu_3tpy)Cl]OTf$ (250 mg, 0.32 mmol) in CH_2Cl_2 (30 mL). The resultant solution was stirred at room temperature for 5 h. After removal of solvent, the residue was purified by column chromatography on silica gel by using dichloromethane/acetone (3:1 v/v) as the eluent. Subsequent recrystallization by diffusion of diethyl ether into a dichloromethane solution of the product gave **1** as an orange solid (260 mg, 80%). ^1H NMR (300 MHz, CD_3CN, 333 K): δ = 1.50 (s, 18H; *tert*-butyl), 1.60 (s, 9H; *tert*-butyl), 7.24 (dt, J = 1.5 and 6.6 Hz, 2H, carbazole), 7.40 (m, 4H, carbazole), 7.63 (d, J = 8.6 Hz, 2H, phenyl), 7.79 (d, J = 8.6 Hz, 2H, phenyl), 8.00 (dd, J = 2.1 and 6.0 Hz, 2H, terpyridyl), 8.14 (d, J = 7.7 Hz, 2H, carbazole), 8.73 (d, J = 2.0 Hz, 2H, terpyridyl), 8.80 (s, 2H, terpyridyl), 9.28 (d with Pt satellite, J = 6.0 Hz, J_{Pt-H} = 45 Hz, 2H, terpyridyl). IR (nujol, ν/cm^{-1}): 2115 (w) ν(C≡C). Positive FAB-MS: m/z 863 $[M-OTf]^+$. Elemental analysis calcd (%) for $C_{48}H_{47}F_3N_4O_3PtS\cdot 1/2H_2O$: C 56.47, H 4.61, N 5.49; found: C 56.51, H 4.62, N 5.45.

Scheme 1. Structure of $[Pt(^tBu_3tpy)(C{\equiv}C{-}C_6H_4\text{-}4\text{-carbazole-}9)](OTf)$ 1

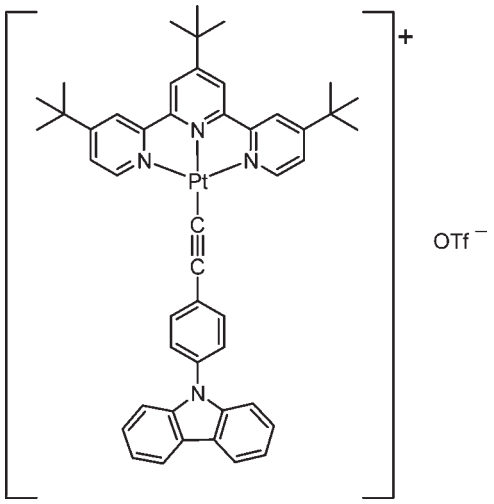

Apparatus. All electrochemical measurements were performed with the CH Instruments model 600A electrochemical workstation. The three-electrode system consisted of a working electrode (0.0707 cm^2), a coiled Pt wire counter electrode, and a saturated calomel electrode (SCE) or Ag/AgCl reference electrode. The ECL signals were measured with a photomultiplier tube (PMT, Hamamatsu R928) installed under the electrochemical cell. A voltage of −800 V was supplied to the PMT with the Sciencetech PMH-02 instrument (Sciencetech Inc., Hamilton, Ontario, Canada). A 3-mm diameter glassy carbon (GC) electrode, gold electrode, and platinum electrode were polished with 0.05-μm alumina slurry to obtain a mirror surface and then were sonicated and thoroughly rinsed with ultrapure deionized water. Before measurement in the aprotic solution, the GC electrode was rinsed with MeCN followed by drying in an oven at 50 °C for 10 min. Before each experiment, the gold and platinum electrodes were subjected to repeated scanning in a wide potential range in 0.1 M H_2SO_4 solution until reproducible voltammograms were obtained. To eliminate the influence of oxygen, all solutions were deaerated by bubbling high purity (99.995%) N_2, and a constant flow of N_2 was maintained over the solution during the measurements. All potentials reported were against the SCE reference with the aprotic system using ferrocene as an internal standard ($E°$(ferrocene$^{+/0}$) = +0.424 V vs SCE).[23] All experiments were performed at room temperature.

UV−visible spectra were obtained on a Hewlett-Packard 8452A diode array spectrophotometer. PL spectral measurements were performed on a Spex Fluorolog-2 model F 111 spectrofluorometer, equipped with a Hamamatsu R928 photomultiplier tube detector. ECL spectral measurements were conducted by using an Oriel InstaSpec V intensified charged-coupled device camera system (model 77195) cooled to −15 °C. Luminescence quantum yield of sample **1** in 0.15 M phosphate buffer (PB) solution (pH 7, 25% MeCN) was measured by the optical dilute method reported by Demas and Crosby,[24] using $[Ru(bpy)_3]Cl_2$ as the standard.[25] Excited-state lifetime of sample **1** in the solution mixture was measured using a conventional laser system. The excitation source used was the 355-nm output (third harmonic, 8 ns) of a Spectra-Physics Quanta-Ray Q-switched GCR-150 pulsed Nd:

Table 1. Crystallographic and Structural Refinement Data for Complex 1

empirical formula	$C_{48}H_{47}F_3N_4O_3PtS$
formula weight	1012.05
temperature	301(2) K
wavelength	0.71073 Å
crystal system	orthorhombic
space group	*Pbca*
unit cell dimensions	a = 19.126(4) Å
	b = 19.592(4) Å
	c = 24.351(5) Å
volume	9125(3) Å^3
Z	8
density (calculated)	1.473 g cm^{-3}
absorption coefficient	3.178 mm^{-1}
F(000)	4064
Crystal size	0.30 mm ×0.25 mm ×0.20 mm
data collection range	1.98 to 25.68°
index ranges	$-13 \le h \le 23$
	$-22 \le k \le 23$
	$-29 \le l \le 27$
reflections collected	44672
independent reflections	8660 [R(int)[a] = 0.0295]
completeness to θ = 25.35°	100.0%
absorption correction	none
refinement method	full-matrix least-squares on F^2
data/restraints/parameters	8660/0/550
goodness-of-fit[b] on F^2	1.124
final R indices [$I > 2\sigma(I)$][c]	$R1$ = 0.0330, $wR2$ = 0.0646
R indices (all data)	$R1$ = 0.0537, $wR2$ = 0.0760
largest diff. peak and hole	1.282 and −1.225 e Å^{-3}

[a] $R_{int} = \Sigma|F_o^2 - F_o^2(\text{mean})|/\Sigma[F_o^2]$. [b] GoF = $\{\Sigma[w(F_o^2 - F_c^2)^2]/(n-p)\}^{1/2}$, where n is the number of reflections and p is the total number of parameters refined. The weighting scheme is: $w = 1/[\sigma^2(F_o^2) + (aP)^2 + bP]$, where P is $[2F_c^2 + \text{Max}(F_o^2, 0)]/3$. [c] $R1 = \Sigma||F_o| - |F_c||/\Sigma|F_o|$, $wR2 = \{\Sigma[w(F_o^2 - F_c^2)^2]/\Sigma[w(F_c^2)^2]\}^{1/2}$.

YAG laser (10 Hz). Luminescence decay signals were recorded on a Tektronix Model TDS-620A (500 MHz, 2 GS/s) digital oscilloscope and analyzed using a program for exponential fits.

X-ray Crystal Structure Determination. Single crystals of **1** were obtained by diffusion of *n*-hexane into an acetone solution of the complex. A crystal of dimensions 0.30 mm ×0.25 mm ×0.20 mm mounted in a glass capillary was used for data collection at 301 K on a Bruker Smart CCD 1000 using graphite monochromatized Mo−K_α radiation (λ = 0.71073 Å). The structure was solved by direct methods employing SHELXS 97 program.[26] The Pt, S, and most of the non-hydrogen atoms were located according to direct methods and successive least-squares Fourier cycles. The positions of other non-hydrogen atoms were found after successful refinement by full-matrix least-squares using SHELXL 97.[27] All 8660 independent reflections (R_{int} equals to 0.0295, 6621 reflections larger than $4\sigma(F_o)$) from a total 44672 reflections participated in the full-matrix least-squares refinement against F^2, where $R_{int} = \Sigma|F_o^2 - F_o^2(\text{mean})|/\Sigma[F_o^2]$. These reflections were in the range of $-13 \le h \le 23$, $-22 \le k \le 23$, $-29 \le l \le 27$ with $2\theta_{max}$ equals to 51.36°. One crystallographic asymmetric unit consists of one formula unit. Hydrogen atoms were generated using SHELXL 97, and their positions were calculated based on the riding mode with thermal parameters equal to 1.2 times that of associated C atoms, and were participated in the calculation of the final R-indices. Convergence $((\Delta/\sigma)_{max} = 0.001$, av. 0.001) for 550 variable parameters by full-matrix least-squares refinement on F^2 reaches to $R_1 = 0.0330$ and $wR_2 = 0.0646$ with a goodness-of-fit of 1.124. Crystallographic and structural refinement data are given in Table 1.

RESULTS AND DISCUSSION

Crystal Structure Determination. The perspective drawing of the complex cation of **1** is shown in Figure 1a. Selected bond distances and bond angles are tabulated in Table 2. The platinum(II) center, coordinated to a terpyridyl and an alkynyl group, adopts a distorted square planar geometry. Because of the steric demand of the terpyridyl ligand, the N−Pt−N angles [N(1)−Pt(1)−N(2) 80.67°; N(2)−Pt(1)−N(3) 80.55°; N(1)−Pt(1)−N(3) 161.22°] show deviation from the idealized values of 90° and 180°. The bond lengths of Pt−N [Pt(1)−N(1) 2.016 Å; Pt(1)−N(2) 1.955 Å; Pt(1)−N(3) 2.023 Å] are comparable to that of other platinum(II) terpyridyl systems,[15a,d,f,g,19a,b,d,f,g,20,21] while the Pt(1)−C(28) bond of 2.040 Å and C(28)−C(29) of 1.141 Å are in the range typical of platinum(II) alkynyl complexes.[15a,d,f,g,19a,b,d,f,g,20,21] The phenyl ring of the alkynyl ligand is not in coplanar arrangement with respect to the [Pt(tpy)] and carbazole planes, with the interplanar angles of 18.39° and 58.28°, respectively.

Despite the rigidity of the alkynyl group as a result of sp hybridization, it is noteworthy that the linkage about the alkynyl unit is essentially bent [N(2)−Pt(1)−C(28) 178.59°, Pt(1)−C(28)−C(29) 175.1°, and C(28)−C(29)−C(30) 176.7°] to form a chain curvature, probably because of crystal packing forces. The closest Pt···Pt distances (4.207 Å) between adjacent molecules are found to be longer than the sum of van der Waals radii for two platinum(II) centers, suggestive of insignificant Pt···Pt interactions in their crystal lattices. The crystal packing of **1** shows that the two [Pt(tpy)] moieties are stacked in a head-to-tail manner with interplanar distance of 3.18 Å, and are shifted laterally with respect to each other to minimize the mutual repulsion between the sterically bulky tri-*tert*-butylterpyridine ligands (Figure 1b). It is interesting to note that the carbazole plane also stacks with the [Pt(tpy)] plane with interplanar angle and distance of 12.347° and 3.709 Å, respectively.

Electronic Absorption and Photoluminescence. The electronic absorption spectrum of complex **1** in MeCN displays high-energy bands at 200−350 nm and low-energy bands at 350−500 nm at room temperature (Figure 2a). The high-energy absorption bands, with extinction coefficients (ε) on the order of 10^4 dm^3 mol^{-1} cm^{-1}, are assigned as intraligand (IL) $\pi-\pi^*$ (^{t}Bu$_3$tpy) transitions of the terpyridyl ligand;[19] while the less intense low-energy absorption bands, with extinction coefficients (ε) on the order of 10^3 dm^3 mol^{-1}cm^{-1}, are ascribed to dπ(Pt) → π^*(^{t}Bu$_3$tpy) metal-to-ligand charge-transfer (MLCT) transitions, probably with some mixing of a π(C≡CR) → π^*(^{t}Bu$_3$tpy) ligand-to-ligand charge transfer (LLCT) character.[19]

Upon photoexcitation, unlike a number of platinum(II) terpyridyl complexes that display intense emission bands, derived from a dπ(Pt) → π^*(^{t}Bu$_3$tpy) ^{3}MLCT excited state with mixing of a π(C≡CR) → π^*(^{t}Bu$_3$tpy) ^{3}LLCT state,[19] **1** did not display any noticeable emission bands in MeCN at room temperature. Some related complexes, such as [Pt(tpy)(C≡C−C$_6$H$_4$−OMe)]$^+$,[19a] [Pt(bpy)(C≡C−C$_6$H$_4$−OMe)$_2$]$^+$,[19a] and [Pt(tpy)(C≡C−C$_6$H$_4$−NR$_2$)]$^+$,[19h] bearing electron-donating substituents on the alkynyl ligand were also reported to be non-emissive or weakly emissive. The suppressed emission behavior

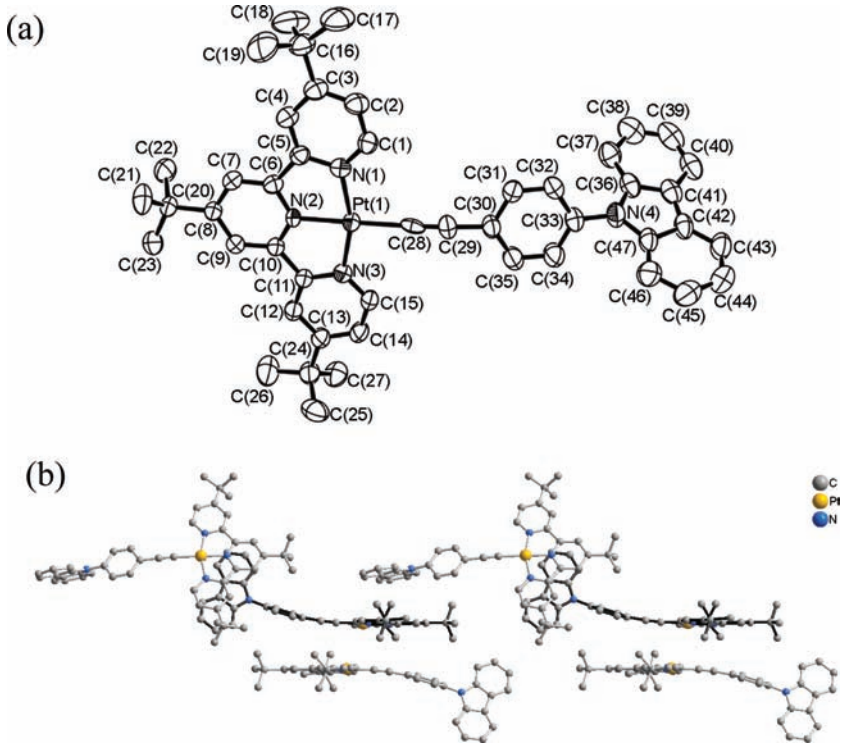

Figure 1. (a) Perspective drawing of the complex cation of **1** with atomic numbering scheme. Hydrogen atoms are omitted for clarity. Thermal ellipsoids are drawn at 50% probability level. (b) Crystal packing diagram of complex cations of **1**.

of these Pt(II) terpyridyl complexes in MeCN solution has been ascribed to the quenching of the ^{3}MLCT state by the lower-lying non-emissive ^{3}LLCT state, as well as by photoinduced electron transfer (PET), in which the electron is transferred from the electron-rich substituent group to the platinum metal center to quench the emissive ^{3}MLCT excited state. Interestingly, dramatic emission enhancement of **1** could be observed at about 620 and 640 nm in 0.15 M PB solution (with 25% MeCN) (Figure 2a) or upon addition of H_2O in MeCN solution at room temperature, respectively. The plot of emission intensity against percentage of PB solution in the solution mixture is shown in Figure 2b, in which the maximum PL intensity could be obtained in 75% PB solution (with 25% MeCN). The emission intensity in 99% PB solution (with 1% MeCN) mixture is of ~90% compared to this maximum PL intensity. In view of the observation of an emission band at similar energy (625 nm) in the solid state at room temperature, the revival of emission is probably due to the formation of nanoaggregates with increasing water composition. Similar aggregation induced emission (AIE) has been reported in other organic systems,[28] and related alkynylplatinum(II) terpyridyl complexes.[19b−e] Because of the presence of the sterically bulky tri-*tert*-butylterpyridine ligand, which would prevent the formation of Pt···Pt or $\pi\cdots\pi$ interactions, the emission origin is suggested to be derived from a dπ(Pt) → π^*(^{t}Bu$_3$tpy) ^{3}MLCT excited state, mixed with a π(C≡CR) → π^*(^{t}Bu$_3$tpy) ^{3}LLCT character, of the nanoaggregates. The luminescence quantum yield of **1** in 0.15 M PB solution (pH 7, 25% MeCN) was found to be 6.3×10^{-3}, measured at room temperature using $[Ru(bpy)_3]^{2+}$ as standard. The lifetime under the same experimental condition was found to be less than 0.1 μs.

Electrochemistry. Figure 3 shows the cyclic voltammograms (CVs) of **1** in acetonitrile (0.1 M ^{n}Bu$_4$NPF$_6$) with scan rates at 100 mV s^{-1}. The result indicates that **1** undergoes two quasi-reversible reduction processes with $i_{p,a}/i_{p,c} = \sim 0.90$ and ~0.85 at $E_{1/2} \sim -0.92$ V and ~ -1.41 V versus SCE, respectively. The two reduction couples could be ascribed to the two successive one-electron reductions of the terpyridyl ligand.[15i,j,19a,19g,19i]

Table 2. Selected Bond Distances (Å) and Bond Angles (deg) for Complex 1 with Estimated Standard Deviations (e.s.d.s.) Given in Parentheses

Bond Distances (Å)			
Pt(1)−N(1)	2.016(4)	Pt(1)−N(2)	1.955(3)
Pt(1)−N(3)	2.023(4)	Pt(1)−C(28)	2.040(5)
C(28)−C(29)	1.141(6)	C(29)−C(30)	1.437(6)
N(4)−C(33)	1.428(6)		
Bond Angles (deg)			
N(1)−Pt(1)−N(2)	80.67(14)	N(2)−Pt(1)−N(3)	80.55(14)
C(28)−Pt(1)−N(1)	99.49(15)	C(28)−Pt(1)−N(3)	99.27(15)
N(1)−Pt(1)−N(3)	161.22(14)	N(2)−Pt(1)−C(28)	178.59(15)
Pt(1)−C(28)−C(29)	175.1(4)	C(28)−C(29)−C(30)	176.7(6)
C(36)−N(4)−C(47)	108.8(4)	C(33)−N(4)−C(47)	126.2(4)
C(33)−N(4)−C(36)	125.0(4)		

In contrast, two irreversible oxidation waves were observed at $\sim +1.22$ and $\sim +1.47$ V,[15i,j] indicating the instability of the oxidation products of **1** probably because of the fast decomposition processes. There is no essential change for the CV profile of **1** upon repetitive scans (>3 cycles) within the studied potential range (+1.8 to −1.9 V).

ECL Using $S_2O_8^{2-}$ as Coreactant. The electrochemical behavior of $S_2O_8^{2-}$ was studied in 0.15 M PB solution (pH 7, 25% MeCN), in which the maximum PL intensity was obtained. As shown in Figure 4, the polished GC electrode is generally free

dx.doi.org/10.1021/ic101119q |*Inorg. Chem.* 2011, 50, 2125–2132

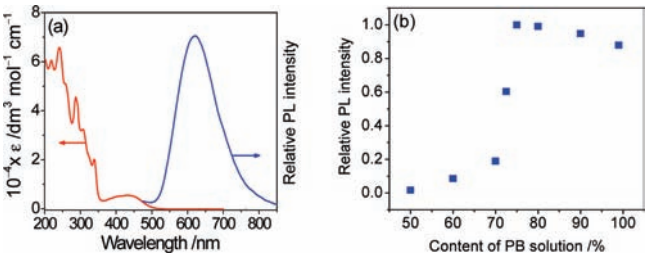

Figure 2. (a) Electronic absorption spectrum of **1** in MeCN (red line) and photoluminescence spectrum of **1** in 0.15 M PB solution (pH 7, 25% MeCN) (blue line). (b) Effect of PB solution (0.15 M, pH 7) content (v/v) in the solution mixture on the photoluminescence intensity. The spectral profile with $\lambda_{max} = \sim 620$ nm is independent of the PB solution percentage from 75%−99%. Note that the phosphate salt would precipitate when the content of PB solution ≤40% (with MeCN ≥ 60%).

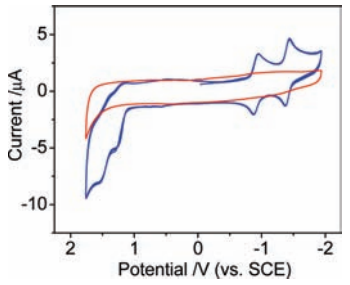

Figure 3. Successive cyclic voltammograms of **1** (200 μM) in MeCN (0.1 M ^{n}Bu$_4$NPF$_6$) at GC electrode (blue line). Scan rate, 100 mV s^{-1}. The red line represents the cyclic voltammogram of GC in blank solution under the same experimental conditions.

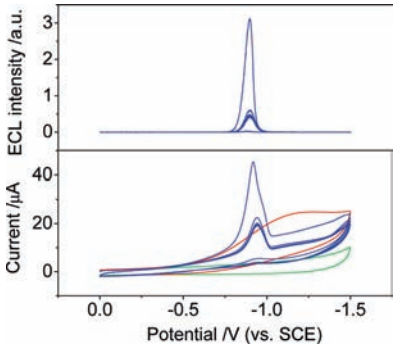

Figure 4. Cyclic voltammograms and corresponding ECL curves obtained at GC electrode (blue line). Solution, **1** (10 μM) and $K_2S_2O_8$ (1.5 mM) in pH 7.0 PBS (0.15 M, 25% MeCN). Scan rate, 100 mV s^{-1}. For comparison, cyclic voltammograms of blank solution (green line) and 1.5 mM $K_2S_2O_8$ (red line) are also presented under the same experimental conditions.

from the interference of H_2 evolution because of the slow proton reduction. Upon addition of 1.5 mM $S_2O_8^{2-}$, a broad cathodic wave corresponding to $S_2O_8^{2-}$ reduction is observed beginning at ∼ −0.20 V. No reoxidation is observed upon scan reversal within the range of scan rates investigated (up to 1 V s^{-1}). The drawn out shape of this wave is attributed to the kinetically slow reduction of $S_2O_8^{2-}$ at the GC surface. A significant current enhancement was observed at −0.92 V when 10 μM of **1** was added to the $S_2O_8^{2-}$ solution. In correlation with the reduction potential of the couple **1**/**1**$^-$, the current enhancement could be

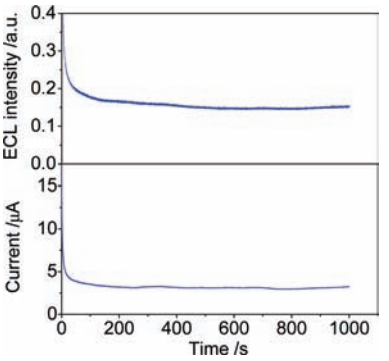

Figure 5. Current and ECL intensity with time obtained at GC electrode. Solution, **1** (10 μM) and $K_2S_2O_8$ (1.5 mM) in 0.15 M PB solution (pH 7, 25% MeCN). The potential was controlled at −0.85 V versus SCE.

interpreted by invoking electrocatalytic reduction of $S_2O_8^{2-}$ by electrogenerated **1**$^-$. The current wave was found to be somewhat sharper than that of a diffusion-controlled reaction, suggesting the involvement of some surface processes, such as adsorption of the reaction products.[29] Correspondingly, the ECL signal began to appear at a potential of ∼ −0.80 V, reaching its maximum intensity at ∼ −0.90 V, which then decreased rapidly upon scanning further toward negative potential, probably because of the substantial consumption of $S_2O_8^{2-}$ near the electrode surface.

Upon successive potential scans, both the oxidation current and the ECL intensity underwent an obvious decrease after the first scan cycle. A relatively stable CV-ECL process was observed in the following cycles. Interestingly, the oxidation current and ECL intensity could almost be recovered to the level of the first cycle if the GC electrode was allowed to stay in solution without holding the potential for several minutes or the solution was stirred or shaken slightly.

The ECL intensity-time profile obtained at GC electrode is shown in Figure 5. When a GC electrode was pulsed from 0.0 to −0.85 V, the ECL intensity decayed quickly, and then it could be kept at a relatively constant level for at least tens of minutes. The result is consistent with that obtained by continuous CV scans as shown in Figure 4, and indicates a dominant diffusion controlled process.

Compared with that of $[Ru(bpy)_3]^{2+/+}$, the potential for redox couple **1**/**1**$^-$ is shifted by about ∼0.55 V toward more positive potential. The ECL based on the reduction of $[Ru(bpy)_3]^{2+}$ (10 μM), where $S_2O_8^{2-}$ (1.5 mM) is also used as coreactant, is nearly unobserved or very weak in aqueous solution or in solutions of high water content because of the instability of $[Ru(bpy)_3]^+$ in the media (see Supporting Information, Figure S1). Upon increasing the content of MeCN to 50%, the ECL intensity of the $[Ru(bpy)_3]^{2+}/S_2O_8^{2-}$ system was found to increase and was ∼2.5-fold that of the **1**/$S_2O_8^{2-}$ system with the same luminophore and $S_2O_8^{2-}$ concentrations in 0.15 M PB solution (pH 7, 25% MeCN). However, the emission was found to appear at a potential of ∼0.65 V more negative compared to that of **1**/$S_2O_8^{2-}$ system and involved a higher content of MeCN.

The ECL of the **1**/$S_2O_8^{2-}$ system was found to be affected by several factors. Experimental conditions, such as the nature of the solvent, pH, and electrode materials could influence the ECL to different extents.

dx.doi.org/10.1021/ic101119q |*Inorg. Chem.* 2011, 50, 2125–2132

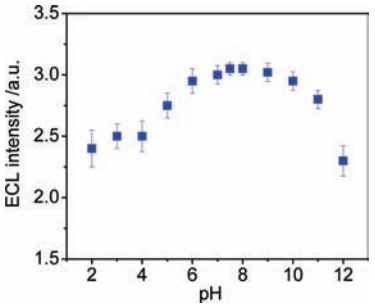

Figure 6. Dependence of ECL intensity on pH obtained at GC electrode. Solution, **1** (10 μM) and $K_2S_2O_8$ (1.5 mM) in 0.15 M PB solution (pH 7, 25% MeCN). Scan rate, 100 mV s^{-1}.

The effect of the nature of the solvent on the ECL was in good agreement with that on the PL. While the ECL intensity was only slightly decreased (10−15%), there was no significant change for the CV-ECL profiles of the $\mathbf{1}/S_2O_8^{2-}$ system upon decreasing MeCN content in the solution mixture down to 1%. As expected, increasing the content of MeCN (>30%) in the solution mixture led to rapid decrease of ECL intensity.

Figure 6 shows the effect of pH on ECL intensity of the $\mathbf{1}/S_2O_8^{2-}$ system. The maximum ECL intensity occurred at around neutral pH. The decrease of the ECL intensity observed in acidic solutions can be explained in part by the consumption of $\mathbf{1}^-$.[30]

$$\mathbf{1}^- + H_3O^+ \rightarrow \mathbf{1} + H_2O + 1/2H_2 \quad (1)$$

Although such a reaction between $\mathbf{1}^-$ and H_3O^+ cannot be totally avoided as suggested by the Nernst equation, the emission decrease observed is not as severe (~ 23% in pH 2) as that of other metal complex/$S_2O_8^{2-}$ systems reported in the acidic media, probably because of the more positive reduction potential of **1**. On the other hand, the decrease of ECL intensity in basic solution was likely ascribed to the consumption of $SO_4^{\bullet-}$, brought about by the scavenging reaction with OH^-.[13c]

$$4SO_4^{\bullet-} + 4OH^- \rightarrow 4SO_4^{2-} + 2H_2O + O_2 \quad (2)$$

ECL of the $\mathbf{1}/S_2O_8^{2-}$ system was also examined with other electrode materials, Au and Pt, as shown in Figure 7. In general, the onset and peak potentials of ECL occur at the same potentials as that at the GC electrode, suggesting the reduction of **1** to $\mathbf{1}^-$ occurs at the same potentials at Au and Pt electrodes. However, the ECL intensity greatly depended on the electrode materials that may be associated in a complicated manner with the hydrogen overpotentials of the electrode materials. At Au electrode, the interference due to the proton reduction that takes place at potentials more negative than −1.0 V seems to be avoided successfully, and comparable ECL intensity is obtained as that at the GC electrode. While most of the studies have been conducted with a GC electrode to minimize the background to aid in the understanding of the mechanism, the use of a gold electrode is important given its extensive use in real analytical applications. At the Pt electrode, however, a redox process was observed appreciably at potentials negative of ~ −0.70 V that is attributed to proton reduction and hydrogen reoxidation. Although the same ECL reaction could occur at the Pt electrode, the continuous evolution of H_2 may greatly interfere with the ECL process, responsible for the decrease in ECL intensity.

Quenching of 1* by $S_2O_8^{2-}$. $S_2O_8^{2-}$ has been widely used as an effective quencher of the excited-state of $[Ru(bpy)]_3^{2+}$,[4b,31] and this system was employed in designing water photolysis cells.[32] Our photoluminescence experiment also revealed a pseudo Stern−Volmer constant K_{SV} of ~2.1 × 10^2 M^{-1} for $\mathbf{1}^*$ by $S_2O_8^{2-}$ in 0.15 M PB solution (pH 7, 25% MeCN). The quenching of $\mathbf{1}^*$ by $S_2O_8^{2-}$ in solution mixture suggests that the ECL efficiency should show a strong dependence on $S_2O_8^{2-}$ concentration. The relative ECL intensity of a 10 μM solution of **1** as a function of $S_2O_8^{2-}$ concentration is shown in Figure 8. The ECL intensity increases with $S_2O_8^{2-}$ concentration up to 1.5−2.0 mM. At higher concentrations, the intensity drops off sharply and is less than 5% of its maximum level at 10 mM $S_2O_8^{2-}$. A further increase in $S_2O_8^{2-}$ concentration completely suppresses the ECL.

ECL Mechanism. As shown in Figure 9, the ECL spectrum is identical to the PL spectrum, indicating that the same $\mathbf{1}^*$ excited state obtained on photoexcitation is also generated in the ECL experiment. By analogy with the known $[Ru(bpy)_3]^{2+}/S_2O_8^{2-}$ system[4] and other metal complex/$S_2O_8^{2-}$ systems,[8−12] the generation of ECL from $\mathbf{1}/S_2O_8^{2-}$ system could be explained by the occurrence of the following reactions:

$$S_2O_8^{2-} + e^- \rightarrow SO_4^{2-} + SO_4^{\bullet-} \quad (E^\circ \leq \sim +0.35 \text{ V vs SCE}) \quad (3)$$

$$\mathbf{1} + e^- \rightarrow \mathbf{1}^- \quad (E^\circ = \sim -0.92 \text{ V vs SCE}) \quad (4)$$

$$\mathbf{1}^- + S_2O_8^{2-} \rightarrow \mathbf{1} + SO_4^{2-} + SO_4^{\bullet-} \quad (5)$$

$$\mathbf{1}^- + SO_4^{\bullet-} \rightarrow \mathbf{1}^* + SO_4^{2-} \quad (6)$$

$$\mathbf{1}^* \rightarrow \mathbf{1} + h\nu \quad (7)$$

The mechanism involves the direct reduction of **1** at the electrode surface, in agreement with the observation that ECL is not observed until reaching potentials where $\mathbf{1}^-$ is produced. Two sources of $SO_4^{\bullet-}$ are possible, namely, that produced directly at the electrode surface (eq 3) and that formed from reaction of $S_2O_8^{2-}$ with $\mathbf{1}^-$ (eq 5). However, because of the immediate reduction of $SO_4^{\bullet-}$ at the electrode, as well as the observation of large catalytic reduction current at the potentials corresponding to the appearance of the ECL signal, eq 5 is probably more important in excited-state production. From the standard electrode potentials of the $SO_4^{\bullet-}/SO_4^{2-}$ (≥+3.15 V vs SCE)[6] and the estimated excited-state reduction potential $E^\circ(\mathbf{1}^{*/-})$ of +1.08 V versus SCE, using spectroscopic $E_{0-0}(\mathbf{1}^{*/0})$ of 2.00 eV and electrochemical data $E^\circ(\mathbf{1}^{0/-})$ of −0.92 V, the minimum free energy of −2.07 eV was calculated from the redox reaction eq 6.

From eq 6, in which removal of one electron from the HOMO−1 of $\mathbf{1}^-$ (corresponding to the same orbital as the highest occupied molecular orbital (HOMO) in **1**) is involved for the generation of the excited state $\mathbf{1}^*$, the function of the carbazole substituent on the alkynyl ligand in the present ECL studies is suggested to be related to the energy level of the HOMO of **1**. No detectable ECL was observed for an analogue of $[Pt(^tBu_3tpy)(C{\equiv}C{-}C_6H_5)]^+$ under the same conditions, probably because of the lower ease of the oxidation for the generation of the excited state with $SO_4^{\bullet-}$, resulting from the lower-lying energy of the HOMO.[33]

Chemiluminescent System. It is expected that chemiluminescence should also be generated under the solution condition similar to that of ECL experiment in the presence of a reductant capable of producing $\mathbf{1}^-$. However, when Al powder or foil

dx.doi.org/10.1021/ic101119q |*Inorg. Chem.* 2011, 50, 2125–2132

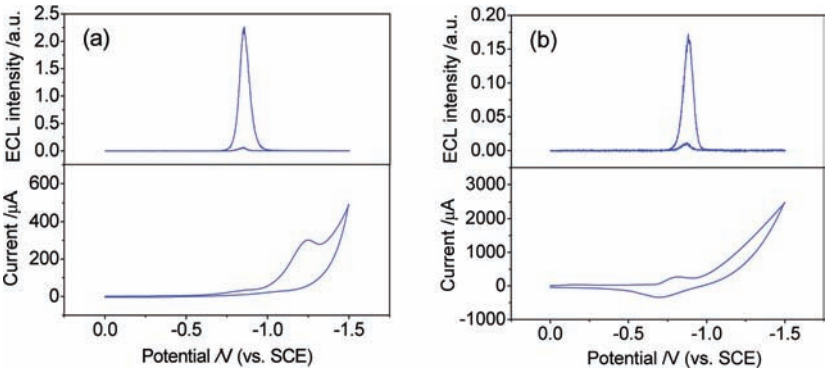

Figure 7. Cyclic voltammograms and corresponding ECL curves obtained at Au (a) and Pt (b) electrodes. Solution, **1** (10 μM) and $K_2S_2O_8$ (1.5 mM) in 0.15 M PB solution (pH 7, 25% MeCN). Scan rate, 100 mV s^{-1}.

($E^o(Al^{3+/0})$ = ~ −1.90 V vs SCE) was added to a 0.15 M PB solution (pH 7, 25% MeCN) of **1** (50 μM) and $K_2S_2O_8$ (7.5 mM), no apparent reaction occured and luminescence was not observed. This is probably due to the Al oxide coating that passivates the Al metal. In contrast, a bright orange emission could be easily observed under dim light when the solution pH was adjusted to 13.0 (see Supporting Information, Figure S2). The initial luminescence was weak, and it started to increase upon dissolving the Al oxide coating and exposing the inner Al metal. The decay of the luminescence on the longer time-scale is probably due to the consumption of the reagents ($S_2O_8^{2-}$ and Al) and the decrease of solution pH. Although the Al oxide coating could also be removed in acidic media, however, the observed emission is not as intense as that under basic conditions. Analogous chemiluminescent system involving $[Ru(bpy)_3]^{2+}$, $S_2O_8^{2-}$, and a stronger reductant (Mg powder) has also been reported.[4b] The production of chemiluminescence presumably follows a pathway similar to that discussed for the ECL, with the external circuit and electrode replaced by a strong electron donor.

CONCLUSIONS

An alkynylplatinum(II) terpyridyl complex tethered with a carbazole moiety, **1**, has been synthesized and characterized. The photophysical and electrochemical behaviors have also been investigated. Such complex was found to show intense ECL using $S_2O_8^{2-}$ as coreactant. The proposed ECL mechanism involves catalytic reduction of $S_2O_8^{2-}$ by electrogenerated $\mathbf{1}^-$ to produce a strongly oxidizing intermediate, $SO_4^{\bullet-}$, that is sufficiently energetic to oxidize $\mathbf{1}^-$ to generate the excited state **1***. Because of a less negative redox potential of $\mathbf{1}^0/^-$ (−0.92 V), the potential of ECL emission of the $\mathbf{1}/S_2O_8^{2-}$ system is significantly shifted by ~0.65 V toward more positive potentials, when compared to that of the $[Ru(bpy)_3]^{2+}/S_2O_8^{2-}$ system. This could prove valuable for ECL applications in the specific determination of $S_2O_8^{2-}$ or as potential ECL labels particularly for those demanding specific biological activities in water.

ASSOCIATED CONTENT

Supporting Information. Crystallographic data of **1** in CIF format. Cyclic voltammograms and corresponding ECL curves of $[Ru(bpy)_3]^{2+}$ using $K_2S_2O_8$ as coreactant in 0.15 M PB solution (pH 7, 1% or 25% MeCN) at GC electrode. Chemiluminescence of $\mathbf{1}/S_2O_8^{2-}$ system in the presence of Al metal with time. This material is available free of charge via the Internet at http://pubs.acs.org.

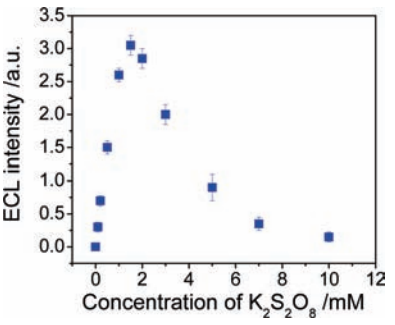

Figure 8. Relative ECL intensity (10 μM **1**) as a function of $K_2S_2O_8$ concentration in 0.15 M PB solution (pH 7, 25% MeCN) at GC electrode. Scan rate, 100 mV s^{-1}.

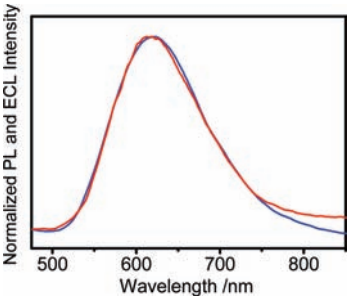

Figure 9. Photoluminescence spectrum of **1** (blue line) and ECL spectrum of $\mathbf{1}/S_2O_8^{2-}$ system (red line) in 0.15 M PB solution (pH 7, 25% MeCN).

AUTHOR INFORMATION

Corresponding Author

*E-mail: wwyam@hku.hk.

ACKNOWLEDGMENT

We acknowledge support from The University of Hong Kong under the Distinguished Research Achievement Award Scheme and the URC Strategic Research Theme on Molecular Materials.

This work has been supported by the University Grants Committee Areas of Excellence Scheme (AoE/P-03/08) and a General Research Fund (GRF) from the Research Grants Council of Hong Kong Special Administrative Region, China (HKU 7076/10P). Z.-F.C. and E.C.-H.K. acknowledge the receipt of postgraduate studentships from The University of Hong Kong.

REFERENCES

(1) (a) Bard, A. J. *Electrogenerated Chemiluminescence*; Marcel Dekker: New York, 2004. (b) Richter, M. M. *Chem. Rev.* **2004**, *104*, 3003. (c) Miao, W. J. *Chem. Rev.* **2008**, *108*, 2506. (d) Knight, A. W. *TrAC, Trends Anal. Chem.* **1999**, *18*, 47. (e) Fähnrich, K. A.; Pravda, M.; Guilbault, G. G. *Talanta* **2001**, *54*, 531.

(2) Leland, J. K.; Powell, M. J. *J. Electrochem. Soc.* **1990**, *137*, 3127.

(3) (a) Chang, M.-M.; Saji, T.; Bard, A. J. *J. Am. Chem. Soc.* **1977**, *99*, 5399. (b) Rubinstein, I.; Bard, A. J. *J. Am. Chem. Soc.* **1981**, *103*, 512.

(4) (a) Bolletta, F.; Ciano, M.; Balzani, V.; Serpone, N. *Inorg. Chim. Acta* **1982**, *62*, 207. (b) White, H. S.; Bard, A. J. *J. Am. Chem. Soc.* **1982**, *104*, 6891.

(5) (a) Zu, Y.; Bard, A. J. *Anal. Chem.* **2000**, *72*, 3223. (b) Kanoufi, F.; Zu, Y.; Bard, A. J. *J. Phys. Chem. B* **2001**, *105*, 210. (c) Miao, W.; Choi, J. P.; Bard, A. J. *J. Am. Chem. Soc.* **2002**, *124*, 14478. (d) Honda, K.; Yoshimura, M.; Rao, T. N.; Fujishima, A. *J. Phys. Chem. B* **2003**, *107*, 1653. (e) Cross, E. M.; Pastore, P.; Wightman, R. M. *J. Phys. Chem. B* **2001**, *105*, 8732. (f) Zhou, M.; Heinze, J.; Borgwarth, K.; Grover, C. P. *Chem. Phys. Chem.* **2003**, *4*, 1241. (g) Liu, X.; Shi, L.; Niu, W.; Li, H.; Xu, G. *Angew. Chem., Int. Ed.* **2007**, *46*, 421. (h) Chen, Z.; Zu, Y. *J. Phys. Chem. C* **2008**, *112*, 16663. (i) Staffilani, M.; Hoss, E.; Giesen, U.; Schneider, E.; Hartl, F. E.; Josel, H. P.; De Cola, L. *Inorg. Chem.* **2003**, *24*, 7789.

(6) Memming, R. *J. Electrochem. Soc.* **1969**, *116*, 785.

(7) Wightman, R. M.; Forry, S. P.; Maus, R.; Badocco, D.; Pastore, P. *J. Phys. Chem. B* **2004**, *108*, 19119 and references therein.

(8) Ouyang, J.; Zietlow, T. C.; Hopkins, M. D.; Fant, F. R. E.; Gray, H. B.; Bard, A. J. *J. Phys, Chem.* **1986**, *90*, 3841.

(9) Richter, M. M.; Bard, A. J. *Anal. Chem.* **1996**, *68*, 2641.

(10) Richter, M. M.; Bard, A. J.; Kim, W.; Schmehl, R. H. *Anal. Chem.* **1998**, *70*, 310.

(11) Wang, H.; Xu, G.; Dong, S. *Microchem. J.* **2002**, *72*, 43.

(12) (a) Kim, J.; Fan, F. F.; Bard, A. J.; Che, C.-M.; Gray, H. B. *Chem. Phys. Lett.* **1985**, *121*, 543. (b) Bonafede, S.; Ciano, M.; Bolletta, F.; Balzani, V.; Chassot, L.; Zelewsky, A. V. *J. Phys. Chem.* **1986**, *90*, 3836.

(13) (a) Gonzales-Velasco, J.; Rubinstein, I.; Crutchley, R. J.; Lever, A. B. P.; Bard, A. J. *Inorg. Chem.* **1983**, *22*, 822. (b) Yamazaki-Nishida, S.; Harima, Y.; Yamashita, K. *J. Electroanal. Chem.* **1990**, *283*, 455. (c) Yamashita, K.; Yamazaki-Nishida, S.; Harima, Y.; Segawa, A. *Anal. Chem.* **1991**, *63*, 872. (d) González-Velasco, J. *J. Phys. Chem.* **1988**, *92*, 2202.

(14) (a) Miskowski, V. M.; Houlding, V. H. *Inorg. Chem.* **1989**, *28*, 1529. (b) Miskowski, V. M.; Houlding, V. H. *Inorg. Chem.* **1991**, *30*, 4446. (c) Houlding, V. H.; Miskowski, V. M. *Coord. Chem. Rev.* **1991**, *111*, 145. (d) Zuleta, J. A.; Burbery, M. S.; Eisenberg, R. *Coord. Chem. Rev.* **1990**, *97*, 47. (e) Chan, C. W.; Cheng, L. K.; Che, C. M. *Coord. Chem. Rev.* **1994**, *132*, 87. (f) Connick, W. B.; Henling, L. M.; Marsh, R. E.; Gray, H. B. *Inorg. Chem.* **1996**, *35*, 6261. (g) Buss, C. E.; Anderson, C. E.; Pomije, M. K.; Lutz, C. M.; Britton, D.; Mann, K. R. *J. Am. Chem. Soc.* **1998**, *120*, 7783. (h) Muro, M. L.; Diring, S.; Wang, X.; Ziessel, R.; Castellano, F. N. *Inorg. Chem.* **2008**, *47*, 6796. (i) Williams, J. A. G. *Top. Curr. Chem.* **2007**, *281*, 205.

(15) (a) Yip, H. K.; Cheung, L. K.; Cheung, K. K.; Che, C. M. *J. Chem. Soc., Dalton Trans.* **1993**, 2933. (b) Aldridge, T. K.; Stacy, E. M.; McMillin, D. R. *Inorg. Chem.* **1994**, *33*, 722. (c) Bailey, J. A.; Hill, M. G.; Marsh, R. E.; Miskowski, V. M.; Schaefer, W. P.; Gray, H. B. *Inorg. Chem.* **1995**, *34*, 4591. (d) Büchner, R.; Cunningham, C. T.; Field, J. S.; Haines, R. J.; McMillin, D. R.; Summerton, G. C. *J. Chem. Soc., Dalton Trans.* **1999**, 711. (e) McMillin, D. R.; Moore, J. J. *Coord. Chem. Rev.* **2002**, *229*, 113. (f) Yam, V. W. W.; Tang, R. P. L.; Wong, K. M. C.; Lu, X. X.; Cheung, K. K.; Zhu, N. *Chem.—Eur. J.* **2002**, *8*, 4066. (g) Puntoriero, F.; Campagna, S.; Di Pietro, M. L.; Giannetto, A.; Cusumano, M. *Photochem. Photobiol. Sci.* **2007**, *6*, 357. (h) Wang, P.; Leung, C.-H.; Ma, D.-L.; Yan, S.-C.; Che, C.-M. *Chem.—Eur. J.* **2010**, *16*, 6900. (i) Field, J. S.; Haines, R. J.; Ledwaba, L. P.; McGuire, R., Jr.; Munro, O. Q.; Low, M. R.; McMillin, D. R. *Dalton Trans.* **2007**, *2*, 192. (j) Michalec, J. F.; Bejune, S. A.; Cuttell, D. G.; Summerton, G. C.; Gertenbach, J. A.; Field, J. S.; Haines, R. J.; McMillin, D. R. *Inorg. Chem.* **2001**, *40*, 2193.

(16) (a) Lippard, S. J. *Acc. Chem. Res.* **1978**, *11*, 211. (b) Jennette, K. W.; Gill, J. T.; Sadownick, J. A.; Lippard, S. J. *J. Am. Chem. Soc.* **1976**, *98*, 6159. (c) Peyratout, C. S.; Aldridge, T. K.; Crites, D. K.; McMillin, D. R. *Inorg. Chem.* **1995**, *34*, 4484. (d) Che, C. M.; Ma, D. L. *Chem.—Eur. J.* **2003**, *9*, 6133. (e) Fuertes, M. A.; Alonso, C.; Pérez, J. M. *Chem. Rev.* **2003**, *103*, 645.

(17) (a) Jamieson, E. R.; Lippard, S. J. *Chem. Rev.* **1999**, *99*, 2467. (b) Che, C. M.; Yang, M.; Wong, K. H.; Chan, H. L.; Lam, W. *Chem.—Eur. J.* **1999**, *5*, 3350.

(18) Ratilla, E. M. A.; Brothers, H. M.; Kostić, N. M. *J. Am. Chem. Soc.* **1987**, *109*, 4592.

(19) (a) Yam, V. W. W.; Tang, R. P. L.; Wong, K. M. C.; Cheung, K. K. *Organometallics* **2001**, *20*, 4476. (b) Yam, V. W. W.; Wong, K. M. C.; Zhu, N. *J. Am. Chem. Soc.* **2002**, *124*, 6506. (c) Yu, C.; Wong, K. M. C.; Chan, K. H. Y.; Yam, V. W. W. *Angew. Chem., Int. Ed.* **2005**, *44*, 791. (d) Yam, V. W. W.; Chan, K. H. Y.; Wong, K. M. C.; Zhu, N. *Chem.—Eur. J.* **2005**, *11*, 4535. (e) Yu, C.; Chan, K. H. Y.; Wong, K. M. C.; Yam, V. W. W. *Proc. Natl. Acad. Sci. U.S.A.* **2006**, *103*, 19652. (f) Yam, V. W. W.; Wong, K. M. C.; Zhu, N. *Angew. Chem., Int. Ed.* **2003**, *42*, 1400. (g) Wong, K. M. C.; Tang, W. S.; Chu, B. W. K.; Zhu, N.; Yam, V. W. W. *Organometallics* **2004**, *23*, 3459. (h) Wong, K. M. C.; Tang, W. S.; Lu, X. X.; Zhu, N.; Yam, V. W. W. *Inorg. Chem.* **2005**, *44*, 1492. (i) Shikhova, E.; Danilov, E. O.; Kinayyigit, S.; Pomestchenko, I. E.; Tregubov, A. D.; Camerel, F.; Retaileau, P.; Ziessel, R.; Castellano, F. N. *Inorg. Chem.* **2007**, *46*, 3038.

(20) Chakraborty, S.; Wadas, T. J.; Hester, H.; Schmehl, R.; Eisenberg, R. *Inorg. Chem.* **2005**, *44*, 6865.

(21) Wadas, T. J.; Wang, Q.-M.; Kim, Y.-J.; Flaschenreim, C.; Blanton, T. N.; Eisenberg, R. *J. Am. Chem. Soc.* **2004**, *126*, 16841.

(22) Sanda, F.; Kawaguchi, T.; Masuda, T.; Kobayashi, N. *Macromolecules* **2003**, *36*, 2224.

(23) Masui, M.; Sayo, H.; Tsuda, Y. *J. Chem. Soc. B* **1968**, 973.

(24) Demas, J. N.; Crosby, G. A. *J. Phys. Chem.* **1971**, *75*, 991.

(25) Caspar, J. V.; Meyer, T. J. *J. Am. Chem. Soc.* **1983**, *105*, 5583.

(26) SHELXS 97; Sheldrick, G. M. *Programs for Crystal Structure Analysis*, Release 97-2; University of Göttingen: Göttingen, Germany, 1997.

(27) SHELXL 97; Sheldrick, G. M. *Programs for Crystal Structure Analysis*, Release 97-2; University of Göttingen: Göttingen, Germany, 1997.

(28) (a) Luo, J.; Xie, Z.; Lam, J. W. Y.; Cheng, L.; Chen, H.; Qiu, C.; Kwok, H. S.; Zhan, X.; Liu, Y.; Zhu, D.; Tang, B. Z. *Chem. Commun.* **2001**, 1740. (b) Chen, J.; Xie, Z.; Lam, J. W. Y.; Law, C. C. W.; Tang, B. Z. *Macromolecules* **2003**, *36*, 1108.

(29) The observations of relative stable CV-ECL signals in Figures 4 and 5 indicate the transient nature of the adsorption.

(30) Nishida, S.; Harima, Y.; Yamashita, K. *Inorg. Chem.* **1989**, *28*, 4073.

(31) Boletta, F.; Juris, A.; Maestri, M.; Sandrini, D. *Inorg. Chim. Acta* **1980**, *44*, L175.

(32) (a) Neuman-Spallart, M.; Kalyansundaram, K.; Grätzel, C.; Grätzel, M. *Helv. Chim. Acta* **1980**, *63*, 1111. (b) Humphry-Baker, R.; Lilie, J.; Grätzel, M. *J. Am. Chem. Soc.* **1982**, *104*, 422.

(33) In contrast, other related complexes, such as $[Pt(^tBu_3tpy)(C{\equiv}C\text{-}C_6H_5\text{-}NR_2)]^+$, with stronger electron-donating substituent on the alkynyl group, did not show ECL signal although the energy level of their HOMO is higher-lying than that of **1**. It is envisaged that even though the corresponding excited state may be generated, such excited state may be quenched by the lower-lying non-emissive ^{3}LLCT state, as well as by photoinduced electron transfer (PET), similar to the observation of its non-emissive nature in the solid state in the PL study.